Development of a Wireless Sensor Node for Building Information Management Systems

Noel Bristow[a], Fergus Elliott[a], Joseph O'Mahony[b], Giray Kartopu[c], SJC Irvine[c], Jeff Kettle[a†]

[a]School of Computer Science and Electronic Engineering, Bangor University, Bangor, Wales, UK
[b]School of Engineering, Waterford Institute of Technology, Waterford, Ireland
[c]CSER
[†]Email: j.kettle@bangor.ac.uk

Abstract— **An increasing number of internet of things (IoT) devices are being deployed long term and therefore need to be self-powered in order to reduce maintenance costs. This paper reports on the design and implementation of a low power wireless sensor node for use in a building information management system powered by an organic solar module. Detailed analysis of the power requirements of the various sensors and the methods used to reduce the power consumption are given. The suitability of organic photovoltaic modules for indoor energy harvesting is examined. Early results from the deployment of these modules are shown.**

Keywords— *organic photovoltaics (OPV), wireless sensor network, internet of things (IoT), low power, energy harvesting.*

I. INTRODUCTION

Over the last 10 years there has been increasing attention on new sensor technologies to enable smart buildings. This could enable buildings based on sustainable construction standards to consume less energy than traditional buildings and to minimize their impact on the natural environment. To achieve this, the application of IoT devices in all spheres of building information modelling could be applied to improve real-time decision making and understand long term trends in energy consumption. IoT devices can consist of a broad array of sensors which can be used to maximise a building's efficiency, reduce energy consumption and increase sustainability. These sensors report environmental conditions back to a centralised building information management system (BIMS), which in turn can control heating, ventilation and air conditioning systems to maintain optimal conditions for the occupants and minimise energy usage. Sensor data can be collected and contextualized in reference to the building information model and can be used as inputs of continuous simulations aiming to predict real-time building energy consumption patterns. Comparing the simulation results against historical performance data via machine learning can further enhance the precision of such models.

However, for such sensor networks to be deployed for long periods of time, energy harvesting is required to make such nodes autonomous, maintenance-free and economically viable [1]. Solar energy harvesting is a method of meeting these requirements and can be used to harvest ambient light indoors to power such sensor nodes and enable smart buildings of the future [2].

II. WIRELESS SENSOR DESIGN

This paper looks at the design and optimisation of an environmental sensor node for incorporation in a BIMS. The sensor node requires three key components; sensors that respond in real-time to report on environmental conditions, ability to communicate to a central system, and to be self-powered. In order to maximise the efficiency of the energy harvesting system it is necessary for the device to be low powered.

A. Microcontroller and Sensors

The node was designed around the ATmega328P microcontroller (MCU), as this allowed rapid prototyping of both the hardware and software. The following sensors were selected, based on their accuracy and minimal use of power:

- BME280 – temperature, humidity and air pressure
- TSL2591 – light (measuring Lux)
- COZIR_A – CO_2 (measuring ppm)
- DS3231 – real time clock (RTC)
- ADS1015 – battery voltage

B. Radio Communication

Two wireless systems were considered to communicate the sensor measurements back to a central control system:

- ZigBee – 2.5GHz, 50-200m range, high data rate.
- LoRaWAN – 868MHz, 2-10km range, very low data rate.

ZigBee has the benefits of a high data rate and being relatively easy to set up in a typical domestic dwelling. It is capable of building mesh networks which can communicate with a single coordinator node connected to a computer running a datalogger program. LoRaWAN on the other hand has a very low data rate, but it does have the advantage over ZigBee of a long range and the ability to use public access gateways. For the initial prototype ZigBee was used as the wireless system. However for future proofing of the system so that it can be used over larger areas such as a small community, LoRaWAN would be a better wireless solution.

C. Low Power Operation

Experiments on early prototypes, along with datasheet specifications, indicated that the highest users of power were the microprocessor, CO_2 sensor and ZigBee wireless module (Table I). The other sensors used very little power in active mode and were all capable of being set to sleep mode. Table I lists the active and sleep mode power consumption of the various components used in our node. During active mode the maximum power consumption was around 165mW; it would be unrealistic to power this continuously using a small solar cell module, so any operation requires sensors to be

periodically set to sleep mode, in order to ensure long-term and autonomous operation.

Component	Active Mode (mW)	Sleep Mode (mW)
ATMega328P	13.2	0.028[a]
DS3231M	0.281	0.281[b]
BME280	0.117	0.014
TSL2591	0.053	0.023
INA226	0.033	0.002
ADS1014	0.495	0.001
ZigBee S2C	148[c]/92[d]	0.001
COZIR_A	3.5[e]	0.029[f]

[a.] Microcontroller in deep-sleep mode

[b.] RTC does not sleep, as it is used to control when the circuit wakes (via interrupt).

[c.] ZigBee operating at maximum transmit power (boost mode).

[d.] ZigBee operating at minimum receive/idle power (normal mode).

[e.] Average operating power of COZIR-A sampling at 2 measurements per second (datasheet) [3].

[f.] COZIR-A powered down by load switch (STMPS2151).

1) Microcontroller

The first target for reducing power consumption was the MCU. Power consumption of the ATMegas328P is closely linked to both voltage and clock frequency [4]. The ATMega328P is capable of being clocked using either an external crystal at frequencies up to 16MHz or an internal crystal at 8MHz. At the higher frequencies it needs to be powered at 5V, but using the internal crystal allows it to work at 3.3V and therefore reduces its power consumption. 3.3V was selected as the voltage for the whole sensor, which will be powered by a 4.2V lithium polymer (LiPo) battery, brought down to 3.3V using an LM367 DC-DC converter, which has a high efficiency and low quiescent current.

The MCU has several sleep modes and initially it was operated using the watchdog timer (WDT) to wake it up. It had been decided to have an on-board real time clock (RTC), so that accurate timestamps could be maintained with each data transmission. In order to keep track of time the RTC cannot be put into sleep mode, so therefore the RTC was used to wake up the MCU. This was achieved by programming the RTC with the required alarm interval and putting the MCU into deep sleep. Once that alarm has been triggered on the RTC it polls an interrupt pin on the MCU and wakes it up.

2) ZigBee Module

The highest power consumption is by the ZigBee module during its transmission cycle. The ZigBee can support two transmission modes: transparent and API. In transparent mode there is a high possibility that simultaneous transmissions from two or more sensor nodes will collide, whereas API mode is packet based and so each transmission will be kept separate. API mode also has the benefit that it supports encryption, allowing the creation of a secure network, which is becoming highly important as these sensors proliferate, and we come to rely on them more and more. The ZigBee has several sleep modes, and the lowest power consumption was obtained using pin-hibernate mode, where the module is woken up be an external signal from the MCU. Only end nodes can sleep, so they will not be able to form the backbone of a mesh network, which has the impact of limiting the range of the network, unless permanently active routers can be placed at strategic locations.

3) CO_2 Sensor

The CO_2 sensor does not have a sleep mode, so a load switch (STMPS2151) was incorporated so that the power could be turned on and off as required by the MCU. The CO_2 sensor can operate in various modes (polling and continuous) and can report both instantaneous and/or filtered measurements at various sampling frequencies (the level of filtering and sampling frequency can be adjusted as required). Figure 1 shows CO_2 measurements taken from a COZIR-A being switched between active and sleep modes, by being powered up/down by an STMPS2151 load switch. The sensor takes a couple of seconds to warm up and then a few seconds for the filtered measurement to settle. The measurement indicated in red is the one being reported back by the sensor.
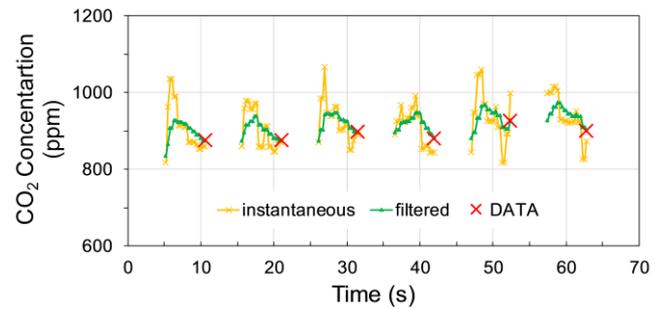

Fig. 1. COZIR-A real time measurements, sampling at 4Hz, filtering=8.

4) Complete Sensor Operation

Figure 2 shows total power consumption over several measurement/transmission cycles (sampling at 1/minute). The average power consumption of the whole sensor has been reduced to 2.27mW.
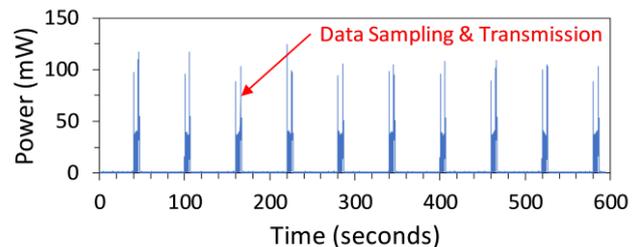

Fig. 2. Power consumption over several measurement/transmission cycles (sampling rate: 1/60 Hz).

Figure 3 shows detail of the power consumption during a single measurement/transmission cycle. The sensor is woken up by the RTC polling an interrupt pin on the MCU, and then powering up the CO_2 sensor, which starts sampling at 2Hz. The MCU then goes back to sleep for 5 seconds while the CO_2 sensor warms up and obtains a filtered measurement. After 5 seconds the MCU wakes up (by RTC interrupt), retrieves the CO_2 measurement and then powers down the CO_2 sensor. The other sensors are then activated, their data retrieved, and de-activated. Once all the measurements are available the ZigBee radio module is activated, and the data transmitted to the network. Finally, the whole sensor is put back in sleep mode, with only the RTC remaining active (with an appropriate alarm set for the duration of the next sleep interval). At the end of the sleep interval the RTC sets an interrupt in the MCU high and the whole process starts again.
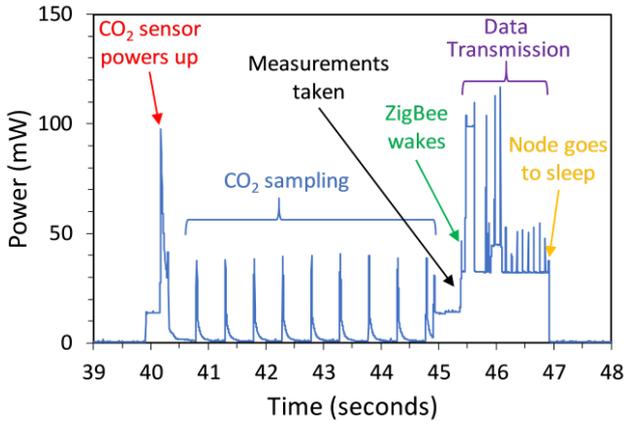
Fig. 3. Detail of power consumption during a single measurement/transmission cycle.

5) *Active Power Management*

In order to further reduce power consumption, active power management techniques are used to control the rate of measurement and transmission. There are several techniques used in this prototype sensor. The first task is to determine the maximum data rate required in an occupied office building when conditions are changing. This has been set at once per minute, so measurements will be taken and transmitted at this rate. If we consider that conditions within an environment like this are unlikely to change very much and that small variations (say less than 5%) are not significant and do not need to be transmitted, we can now measure once a minute and only send if either the data has changed significantly (from the previously transmitted data), or a set interval has passed (say 5 minutes).

A further improvement on this would be to assume that if temperature, light and humidity have not changed significantly, then CO_2 could be assumed to not to have changed and therefore will not be measured. The CO_2 sensor is relatively power hungry, so this would lead to a much-improved energy budget. So, if the office environment was not varying very much only the very low power sensors would be activated frequently and the power consuming CO_2 sensor and RF transceiver would only be activated once every 5 minutes. Another improvement would be to assume that if the sensor was subject to very low light levels then it was unlikely that the room was occupied and therefore the measurement/transmission interval could be extended from 5 minutes to 15 minutes, with the light levels only being monitored every 5 minutes. When the battery voltage indicates that the battery capacity has dropped to below 20% the rate of measurements is reduced to every 30 minutes.
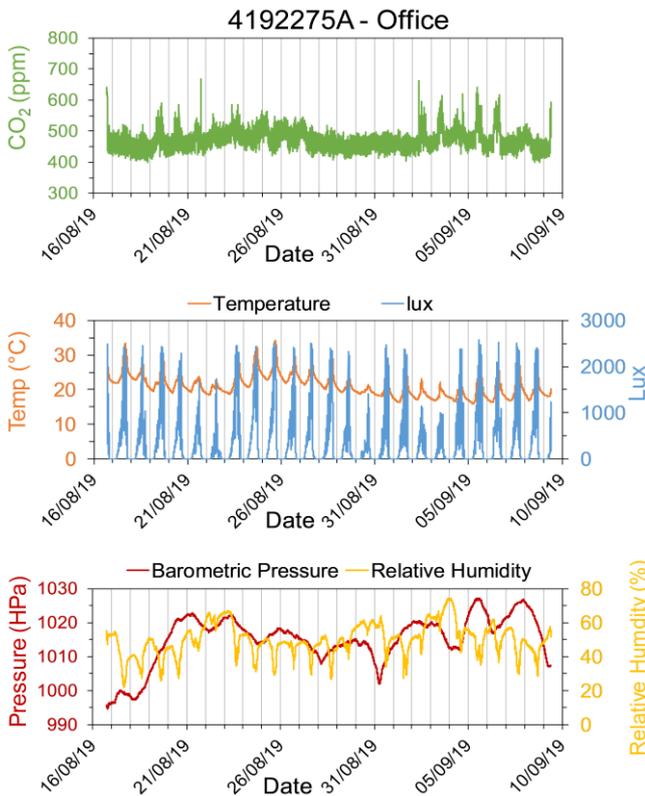

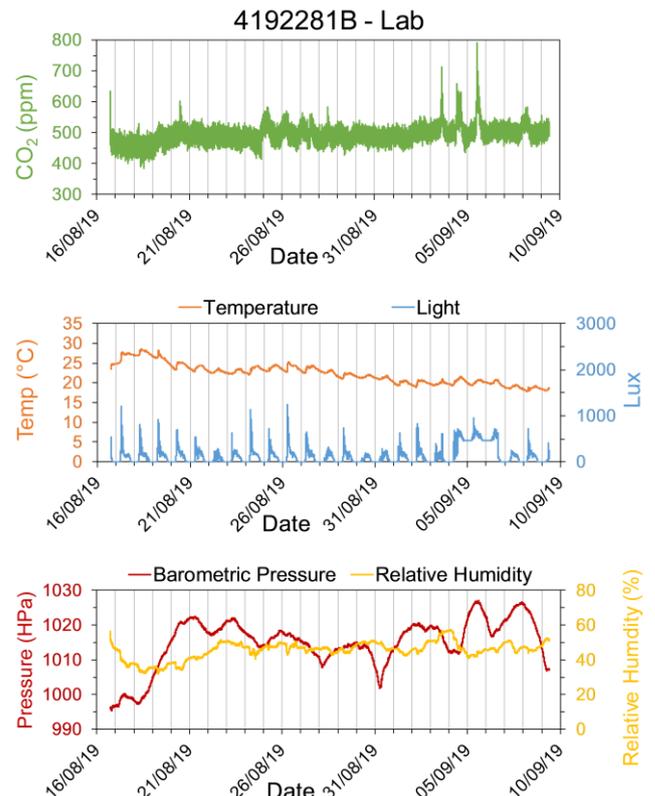Fig. 4. Environmental measurements – south-facing office.

Fig. 5. Environmental measurements – north-facing laboratory.

III. EARLY RESULTS

Two nodes were deployed in a 1960's office building (Department of Electronics, Dean Street, Bangor) in different rooms; south-facing office and north-facing laboratory. The results are shown in figure 4 (office) and figure 5 (laboratory). The office has a higher occupancy rate, and this is reflected in the higher CO_2 and relative humidity readings. The south-facing office is subject to higher levels of sunlight than the north-facing laboratory, and this is reflected in both the higher light levels in the office and the greater temperature fluctuations.

IV. Improvements

Based on these early results there are several improvements that have been made to these nodes:

A. CO₂ sensing

These results show the ±50ppm resolution clearly, the measurements being quite noisy. Despite wanting a quick response to changes in CO_2 levels an improvement is to increase the filtering level to 16 or 32 (the reported measurement being an average of the last x actual measurements). In that case it might be worthwhile only reporting CO_2 levels intermittently, allowing a reduction in power consumption.

B. Communications.

Although the published range for ZigBee modules indoors is ~60m it was found in practice that this the range was much lower (~20m) [5]. ZigBee modules can form mesh networks communicating through various intermediate router nodes to eventually reach the coordinator node. However, this requires the router nodes to be permanently awake, which is too energy intensive to be able to rely on solar energy harvesting for a power source. Therefore, it was decided to use LoRaWAN instead of ZigBee. LoRaWAN is a network stack protocol operating on the LoRa physical layer, operating at 868MHz in Europe [6]. It is low power and has a long range (urban: ~5km), utilizing public gateways to communicate with the internet [7]. The longer range is obtained by using a lower frequency (868MHz) compared to ZigBee (2.5 GHz), and by using chirp spread spectrum modulation, which gives it a much higher receiver sensitivity (down to -146 dBm) [7], [8]. The disadvantage of LoRaWAN is the low data rate and small packet size, but for wireless nodes in BIMS this is not a problem [8].

A LoRaWAN PCB was designed around the RN2483 RF module (from Microchip), with a similar footprint to the ZigBee modules, so that the original ZigBee modules could be replaced in the sensors and only the software needed to be changed [7]. The PCB was designed so that it could be fabricated with either a U.FL or an SMA RF socket, allowing a choice of aerials to be attached (figure 6).
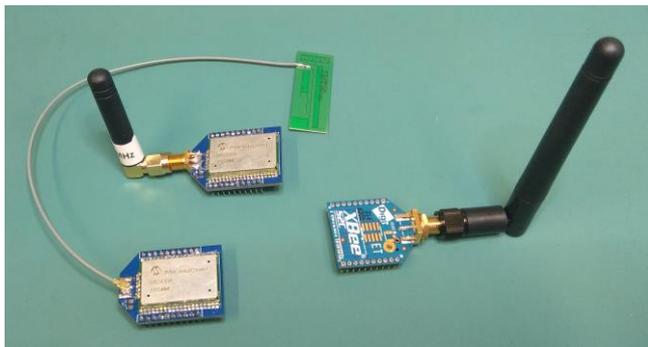

Fig. 6. RF communication modules: On the left are two LoRaWAN modules, (one with a PCB antenna and the other with a stub helical coil). On the right is an XBee ZigBee module from Digi International with a ½ wave dipole antenna.

C. Solar Harvesting

Although the first prototype nodes were powered using a battery the final design requires that they be self-powered. This has been achieved by using a 300mW organic photovoltaic (OPV) module supplied by infinityPV (Denmark). The solar charging is controlled using an SPV1050 MPPT battery charger and an INA226 has been added to measure PV input power.

D. Improved Wireless Sensor Node

Figure 7 shows the improved wireless sensor node, which is currently undergoing tests.

Fig. 7. Wireless sensor node with LoRaWAN RF module powered by an organic solar module.

V. Organic Photovoltaic Modules for Indoor Energy Harvesting

OPVs have the advantage over silicon and thin film PV technologies of ease of processing, low weight, flexibility, semi-transparency, and have a short energy payback time [9], [10]. OPVs have previously been shown to be suitable for indoor energy harvesting and to be more stable indoors due to reduced humidity and UV [11], [12]. Under indoor lighting conditions solar modules are likely to be subject to multiple light sources, leading to shading and reduced light levels. It has previously been shown that under outdoor conditions OPV foil is less affected by shading than expected [13]. A series of experiments were conducted to investigate how different PV technologies responded to these conditions. Three different modules were tested (figure 8): OPV, silicon and thin film CdTe (cadmium telluride). Their characteristics at STC ($1000W/m^2$) are shown in Table II.

Fig. 8. PV module types: a) Silicon, b) CdTe (cadmium telluride), c) OPV.

TABLE II.   CHARACTERISTICS AT STC [AREA IS ACTIVE AREA].

Type	Cells	Area /cm²	Isc /mA	Voc /V	FF	Power /mW	Efficiency
OPV	10	52.0	26.7	4.9	0.39	52	1.0%
Silicon	4	22.9	195.3	2.35	0.69	318	13.9%
CdTe	9	39.2	72.6	5.2	0.44	164	4.2%

A. Effect of Shading

The three PV modules were tested under a solar simulator at $1000W/m^2$, by measuring their IV curve and extracting the principal PV characteristics: I_{SC}, V_{OC}, Power & fill factor (FF). The modules were subjected to two different shading regimes: equal shading where the all of the cells were subjected to equal shading (A) and cell shading where the cells were shaded one by one (B) (figure 9).
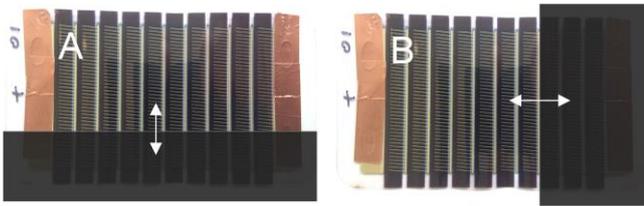
Fig. 9. Shading regimes: A) Equal shading, B) Cell shading.

Figure 10 shows the effect of the different shading regimes on the different PV technologies. Under equal shading (A) all three technologies show similar characteristics, with both V_{OC} and fill factor remaining fairly steady with increasing shading. Both I_{SC} and power exhibit a linear decrease as shading increases. However under unequal cell shading (B) the different technologies perform very differently, as discussed below.
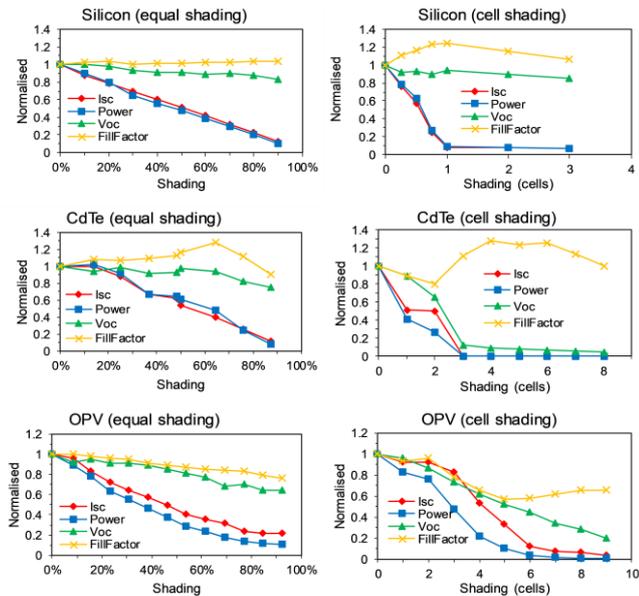

Fig. 10. Effect on I_{SC}, Power, V_{OC} & Fill Factor of equal shading (A) on the left and unequal cell shading (B) on the right.

B. Effect of Low Light Levels

Neutral density film was used to reduce irradiance levels from 100% (1000W/m^2) down to 8% (80W/m^2) in several steps. Figure 11 shows how the three PV technologies are affected by reducing light levels.
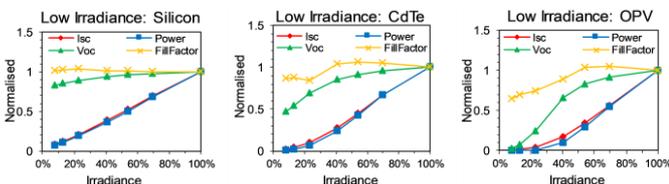

Fig. 11. Effect of reducing irradiance on I_{SC}, Power, V_{OC} & Fill Factor.

C. Discussion of Results

Figure 12 shows a comparison of power output when the modules were subject to equal shading (A). All three PV technologies show a similar linear relationship between shading and power.
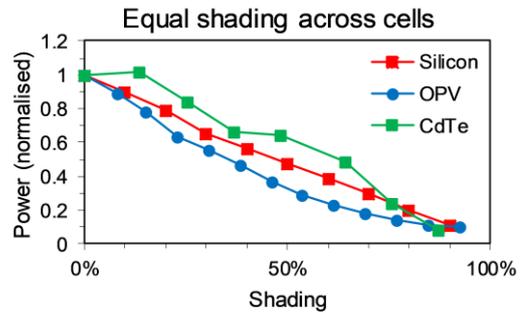

Fig. 12. Comparison between different PV technologies when modules are subjected to equal cell shading (A).

Figure 13 shows a comparison of power output when the modules were subject to unequal cell shading (B). Here the different technologies perform very differently, with silicon exhibiting a 90% drop in power once a single cell is shaded. The effect is less with in CdTe module, which has a 60% loss when a single cell is shaded and 100% loss once 3 cells are shaded. For the OPV modules the loss is much more gradual, only reaching 90% loss once 5 cells are shaded.
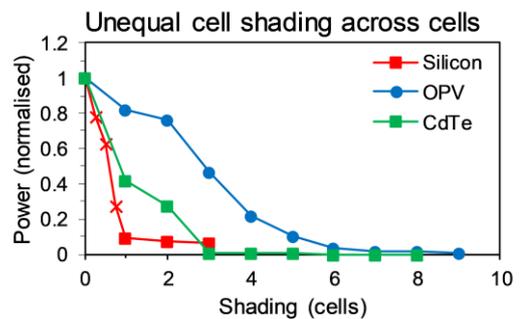

Fig. 13. Comparison between different PV technologies when modules are subjected to unequal cell shading (B).

Figure 14 shows how the different technologies respond to decreasing levels of irradiation. All three show a linear relationship, with OPV performing worst and silicon best.
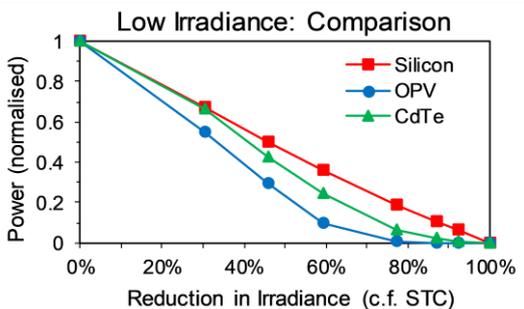

Fig. 14. Comparison between different PV technologies when modules are subjected to decreasing levels of irradiance.

These characteristics all relate to the shunt resistance of the cells: silicon having a very high shunt resistance, leading to cells going into reverse bias once they are fully shaded; OPVs have a relatively low shunt resistance which leads to low fill factor, but allows a module to continue to conduct even when several cells are shaded.

The shading results show that curved OPV modules would be ideally suited to indoor conditions, es and would benefit from the multi-source nature of indoor lighting.

VI. Conclusions

This paper has investigated the development and optimisation of a wireless senor node for use in a building information management system. The initial work concentrated on reducing the power usage and led to further improvements, including the addition of solar energy harvesting using an OPV module. To increase the communication range the original ZigBee module was replaced by a LoRaWAN module. It has been shown that OPVs are suitable for indoor energy harvesting, especially when subjected to shading and low light levels.

References

[1] A. S. Adila, A. Husam, and G. Husi, "Towards the self-powered Internet of Things (IoT) by energy harvesting: Trends and technologies for green IoT," *2018 2nd Int. Symp. Small-Scale Intell. Manuf. Syst. SIMS 2018*, vol. 2018-Janua, pp. 1–5, 2018.

[2] S. Chalasani and J. M. Conrad, "A survey of energy harvesting sources for embedded systems," *Conf. Proc. - IEEE SOUTHEASTCON*, pp. 442–447, 2008.

[3] "CozIR-A Datasheet," 2019. [Online]. Available: https://www.gassensing.co.uk/wp-content/uploads/2019/08/GSS-CozIR-A-Data-Sheet-Keep.pdf. [Accessed: 01-Nov-2019].

[4] Microchip Inc, "ATmega48A/PA/88A/PA/168A/PA/328/P Datasheet - DS40002061A," 2018.

[5] Digi International, "XBee/XBee-PRO S2C Zigbee user guide," 2018.

[6] LoRa Alliance, "LoRaWAN™ 1.0.3 Specification," 2018.

[7] Microchip Inc, "RN2483: Low-power long range LoRa technology transceiver module - datasheet, DS50002346D," 2019.

[8] F. Adelantado, X. Vilajosana, P. Tuset-Peiro, B. Martinez, J. Melia-Segui, and T. Watteyne, "Understanding the limits of LoRaWAN," *IEEE Commun. Mag.*, vol. 55, no. 9, pp. 34–40, 2017.

[9] N. Espinosa, M. Hösel, D. Angmo, and F. C. Krebs, "Solar cells with one-day energy payback for the factories of the future," *Energy Environ. Sci.*, vol. 5, no. 1, pp. 5117–5132, 2012.

[10] B. C. J. Brabec, N. S. Sariciftci, and J. C. Hummelen, "Plastic Solar Cells," *Adv. Funct. Mater.*, vol. 11, no. 1, pp. 15–26, 2001.

[11] H. K. H. Lee, Z. Li, J. R. Durrant, and W. C. Tsoi, "Is organic photovoltaics promising for indoor applications?," *Appl. Phys. Lett.*, vol. 108, no. 25, pp. 1–5, 2016.

[12] J. Kettle, V. Stoichkov, D. Kumar, M. Corazza, S. A. Gevorgyan, and F. C. Krebs, "Using ISOS consensus test protocols for development of quantitative life test models in ageing of organic solar cells," *Sol. Energy Mater. Sol. Cells*, vol. 167, no. April, pp. 53–59, 2017.

[13] F. C. Krebs, N. Espinosa, M. Hösel, R. R. Søndergaard, and M. Jørgensen, "25th anniversary article: Rise to power - OPV-based solar parks," *Adv. Mater.*, vol. 26, no. 1, pp. 29–39, 2014.